OPTIMAL CONTROL WITH FEMTOPULSES: THEORY AND EXPERIMENTS

Fang Gao, Yaoxiong Wang, Dewen Cao and **Feng Shuang**
Institute of Intelligent Machines, Chinese Academy of Sciences, Hefei, China 230031

Jixin Cheng
Weldon School of Biomedical Engineering and Department of Chemistry, Purdue University, West Lafayette, Indiana 47907, USA

Keywords: Femtolaser, Raman scattering, coherence, optical spectroscopy, coherent control, CARS spectroscopy, vibrational levels, Raman effect, quantum interference, chemical bonds, shaping laser pulses, molecular dynamics, 'closed-loop learning' scheme.

Content

1. Introduction
2. Optimal control in coherent anti-Stokes Raman scattering (CARS)
3. Optimal control mechanism analysis
Glossary
Bibliography
Biographical Sketches

Summary

The ideal excitation source for study molecular dynamics, to control the dynamics of atomic, molecular, and solid-state systems, and to drive them into novel, non-equilibrium states is femtosecond laser pulse because of its ultrahigh laser intensity and ultra-short pulse duration. Phase shaping is widely used in femtosecond pulses to achieve the optimal coherent control in femtosecond laser experiments. In the present chapter, two specific applications are taken as examples to demonstrate the potential application of optimal control with femtosecond pulses. One is the optimal control in Coherent Anti-Stokes Raman Scattering (CARS), and control methods can be employed here to improve the chemical selectivity in CARS spectroscopy and spatial resolution in CARS microscopy. The other is about how to obtain the optimal control mechanisms in experiments.

1. Introduction

Femtosecond laser pulse is considered as an ideal excitation source because of its ultrahigh laser intensity and ultrashort pulse duration. As an important technology, femtosecond pulse shaping is to obtain a desired pulse by controlling the pulse amplitude, phase, and polarization direction. Up to now, it has been widely used in the areas of molecular dynamics, nonlinear spectroscopy, femtosecond chemistry, bio-medical imaging and quantum computation (Weiner, 2000; Brif et al, 2010; Goswami, 2003; Weiner, 2011).
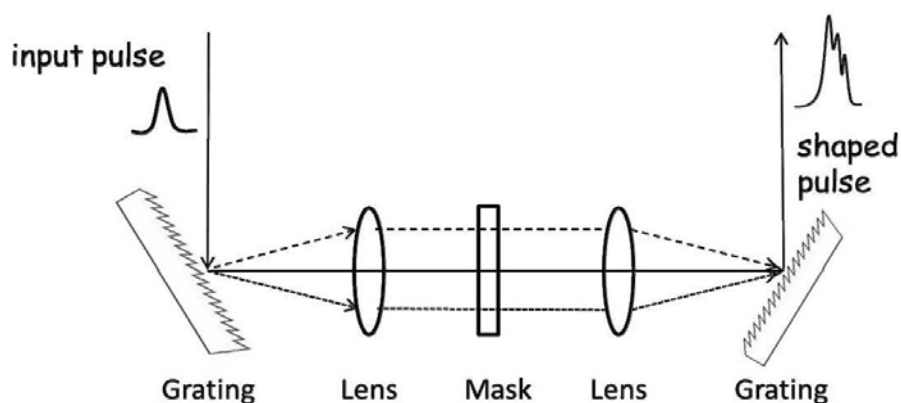
Figure 1. One typical 4-F pulse shaper experimental setup for Fourier Transform pulse shaping.

4-F pulse shaper is mostly commonly adopted as the pulse shaping apparatus in the experiment. As shown in Figure 1, the setup can perform pulse shaping via Fourier Transform. It usually consists of a pair of diffraction gratings and lenses and one mask located in the middle position. The distances between adjacent components are all F , which is the focal length of the lens. That is just why we call this apparatus 4-F pulse shaper. The lenses can also be replaced with concave mirrors, which does not change its principle described in the following. Firstly, the individual frequency components in the input pulse are angularly diffracted by the first grating, and then focused to small diffraction limited spots at the back focal plane of the first lens, where the mask is placed. Thus the frequency components are spatially separated along one dimension in the mask, which can been as a Fourier Transform from the time domain to the frequency domain. Spatially patterned amplitude and phase masks (or a Spatial Light Modulator, SLM) are placed in this plane in order to manipulate the spatially dispersed optical Fourier components.

The pixels in the mask can have different optical properties such as refractive indices to modulate the corresponding incident frequency components. After the mask, the second lens and grating recombine all the frequencies into a single beam to obtain a shaped output pulse. This could be seen as a Fourier Transform from the frequency domain to the time domain. In the 4-F pulse shaper apparatus, the pulse shaping is done via the modulation mask. If the mask performs no modulation, then the output pulse is the same as the input pulse.

Quantum control can be performed with 4-F pulse shaper in femtosecond laser experiments. In the following, two specific applications are taken as examples to demonstrate the potential application of optimal control with 4-F femtosecond pulse shaper. One is the optimal control in coherent anti-Stokes Raman Scattering (CARS), where control methods are employed to improve the chemical selectivity in CARS spectroscopy and spatial resolution in CARS microscopy. The other is about how to obtain the optimal control mechanisms.

Coherent anti-Stokes Raman Scattering, as a four-wave nonlinear process, has been widely used to study chemical systems in solutions, reactions in the gas phase, and

vibrational dynamics in gas and condensed phases. As shown in Figure 2, the pump and Stokes pulses generate coherence between two vibrational levels, when they have a frequency difference which coincides with the Raman resonance Ω_R. The probe pulse then induces the anti-Stokes signal. Thus it can be employed to label biological samples with certain Raman transitions.
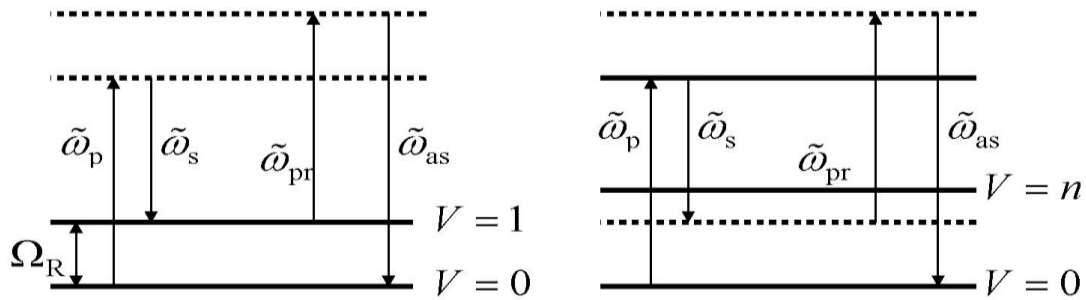

Figure 2. Energy level diagram of the CARS process. The left and right panels correspond to the resonant and non-resonant background contributions, respectively. Three pulses are employed in the process: the pump, Stokes and probe pulses. The solid lines indicate the vibrational levels of the system, while the dotted lines mean virtual states. Reproduced from [Gao et al, 2012], with the permission of AIP Publishing.

CARS microscopy, pioneered by Duncan *et al* (1982) and developed by Xie *et al*, is widely used to image biological species. As a combination of ultrafast nonlinear spectroscopy and microscopy, CARS microscopy is a highly chemically selective and sensitive technique that employs a CARS signal of an unlabeled sample and provides higher spatial resolution. Figure 3 (Cheng et al, 2002) shows four typical configurations of CARS microscopies, and the pulse shaper can of course be added before the first objective lens to modulate the pump or probe pulse. In these microscopies, the pump pulse ω_p is also used as the probe pulse. The temporally and spatially overlapped pump and Stokes laser pulses are tightly focused into a sample to generate a signal in a small excitation volume (<1 μm^3). A CARS image is acquired by raster scanning the sample or the laser beams. The vibrational contrast in CARS microscopy arises from the signal enhancement when $\omega_p - \omega_s$ is tuned to a Raman-active vibrational band.

The femtosecond laser pulse-shaping technique can be integrated into a 'closed-loop learning' scheme to perform quantum control (see Figure 4). The scheme proposed by Judson and Rabitz (1992) has been employed in many femtosecond laser experiments to control the dynamics in a variety of systems of interest. Figure 4 shows a typical 'closed-loop learning' scheme (Rabitz et al, 2000). The loop is entered with an initial field. Then a laser control field design is done by the learning algorithm and the pulse shaper. After that, the modulated pulse will act with the sample in the experiment, and the results will be assessed and fed to the algorithm to suggest an improved field design. These steps are repeated until the objective is achieved. The scheme is a kind of feedback control and can identify the best shapes of femtosecond laser control pulses for steering quantum dynamics towards the desired target. The mechanisms under the

shaped pulses in the experiment are usually complex, and the Rabitz group has proposed a method called Hamiltonian encoding-observable decoding (HE-OD) to unveil the control mechanisms. This method often can be implemented with only software changes guiding the laser apparatus of many "closed-loop learning" experiments, and the details will be given in Section 2.1.
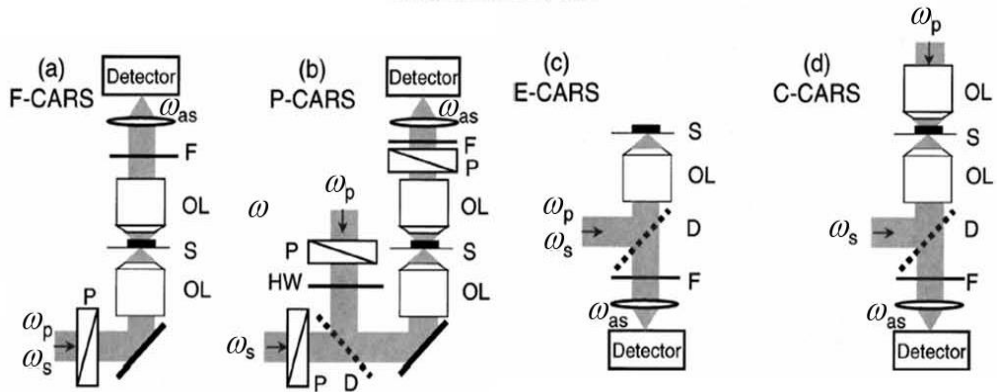

Figure 3. Four types of CARS microscopies: forward-detected CARS (F-CARS), forward-detected polarization CARS (P-CARS), epidetected CARS (E-CARS) and counter-propagating CARS (C-CARS). P, polarizer; OL, objective lens; S, sample; F, filter; HW, half-wave plate; D, dichroic mirror. Reproduced from [Cheng et al, 2002], with the permission of OSA Publishing.
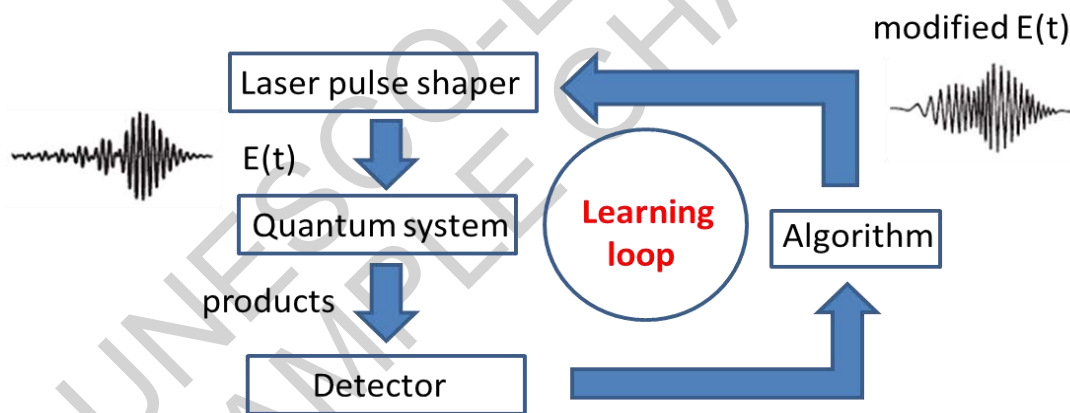

Figure 4. A 'closed-loop learning' scheme for teaching a laser to control quantum systems.

2. Optimal Control in Coherent anti-Stokes Raman Scattering (CARS)

Usually picosecond pulses are used in CARS spectroscopy and microscopy, and its narrow bandwidth is adequate to detect specific Raman bands. Additionally, the non-resonant background is greatly suppressed. However, when investigating broadband CARS spectra, especially in the Raman fingerprint region which spans from 800 to 1800 cm^{-1}, we have to bring in broadband femtosecond pulses. In this case, the non-resonant background may become significant. Therefore, optimal control is necessary

to simultaneously enhance the resonant signal and suppress the non-resonant background (Gao et al, 2012).

2.1. Optimal Control in CARS Spectroscopy

The CARS signal $I_{\text{CARS}}(\tilde{\omega}_{\text{as}})$ is a coherent superposition of resonant third-order nonlinear polarization $P_{\text{r}}^{(3)}(\tilde{\omega}_{\text{as}})$ and non-resonant third-order nonlinear polarization $P_{\text{nr}}^{(3)}(\tilde{\omega}_{\text{as}})$, $I_{\text{CARS}}(\tilde{\omega}_{\text{as}}) = |P_{\text{r}}^{(3)}(\tilde{\omega}_{\text{as}}) + P_{\text{nr}}^{(3)}(\tilde{\omega}_{\text{as}})|^2$ with

$$P_{\text{r}}^{(3)}(\tilde{\omega}_{\text{as}}) = \iint\int_{-\infty}^{\infty} d\tilde{\omega}_{\text{p}} d\tilde{\omega}_{\text{s}} d\tilde{\omega}_{\text{pr}} \frac{C}{\Omega_{\text{R}} - (\tilde{\omega}_{\text{p}} - \tilde{\omega}_{\text{s}}) - i\Gamma} \tilde{E}_{\text{p}}(\tilde{\omega}_{\text{p}}) \tilde{E}_{\text{s}}^{*}(\tilde{\omega}_{\text{s}}) \tilde{E}_{\text{pr}}(\tilde{\omega}_{\text{p}}) \delta(\tilde{\omega}_{\text{as}} - \tilde{\omega}_{\text{p}} + \tilde{\omega}_{\text{s}} - \tilde{\omega}_{\text{pr}})$$

,

$$P_{\text{nr}}^{(3)}(\tilde{\omega}_{\text{as}}) = \iint\int_{-\infty}^{\infty} d\tilde{\omega}_{\text{p}} d\tilde{\omega}_{\text{s}} d\tilde{\omega}_{\text{pr}} \chi_{\text{nr}} \tilde{E}_{\text{p}}(\tilde{\omega}_{\text{p}}) \tilde{E}_{\text{s}}^{*}(\tilde{\omega}_{\text{s}}) \tilde{E}_{\text{pr}}(\tilde{\omega}_{\text{p}}) \delta(\tilde{\omega}_{\text{as}} - \tilde{\omega}_{\text{p}} + \tilde{\omega}_{\text{s}} - \tilde{\omega}_{\text{pr}}).$$

Here Ω_{R} is the Raman frequency between energy levels 1 and 2, 2Γ is the level width, C is a constant which depends on the material property, and χ_{nr} is the non-resonant third-order susceptibility.

The pulses employed in laser experiments are usually of the Gaussian form:

$$\tilde{E}_{k}(\tilde{\omega}_{k}) = \frac{E_{k}}{\Delta_{k}^{1/2}} e^{-(\tilde{\omega}_{k} - \Omega_{k})^2 / \Delta_{k}^2} e^{i\Phi_{k}(\tilde{\omega}_{k} - \Omega_{k})}, k = \{\text{p,s,pr}\},$$

where $2\sqrt{\ln 2}\Delta_{k}$ is the corresponding spectral full width at half maximum (FWHM), and $\Phi_{k}(\tilde{\omega}_{k} - \Omega_{k})$ is the frequency-domain phase profile. For simplicity, the translation $\omega_{k} = \tilde{\omega}_{k} - \Omega_{k}$ is made. Different phase strategies can be adopted to achieve local optimal control or broadband optimal control.

If we just want to maximize the resonant signal or minimize the non-resonant background at $\omega_{\text{as}} = 0$, that is, $\tilde{\omega}_{\text{as}} = \Omega_{\text{as}}$, the answer is easy to be obtained. The first three cases in the following are for this kind of control, namely, local optimal control.

Case 1: All the three pulses are shaped for local optimal control at $\omega_{\text{as}} = 0$. This is the case in three-pulse CARS. We have

$$| P_r^{(3)} | = | \int_{-\infty}^{\infty} \frac{C}{\omega_{pr} - i\Gamma} E_{pr}(\omega_{pr}) [\int_{-\infty}^{\infty} E_p(\omega_p) E_s^*(\omega_p + \omega_{pr}) d\omega_p] d\omega_{pr} |$$

$$= | \frac{1}{\Delta^{3/2}} \int_{-\infty}^{\infty} \frac{C}{\omega_{pr} - i\Gamma} e^{-\frac{3\omega_{pr}^2}{2\Delta^2} + i\Phi_{pr}(\omega_{pr})} A(\omega_p, \omega_{pr}) d\omega_{pr} |$$

$$\leq | \frac{1}{\Delta^{3/2}} \int_{-\infty}^{\infty} \frac{C}{\omega_{pr} - i\Gamma} e^{-\frac{3\omega_{pr}^2}{2\Delta^2} + i\Phi_{pr}(\omega_{pr})} || A(\omega_p, \omega_{pr}) | d\omega_{pr} |$$

$$\leq | \frac{1}{\Delta^{3/2}} \int_{-\infty}^{\infty} \frac{C}{\omega_{pr} - i\Gamma} e^{-\frac{3\omega_{pr}^2}{2\Delta^2} + i\Phi_{pr}(\omega_{pr})} | g \sqrt{\frac{\pi}{2}} \Delta g d\omega_{pr} |$$

$$(\text{when} \quad \Phi_p(\omega_p) = \text{cons}, \quad \Phi_s(\omega_s) = \text{cons})$$

$$\leq C \sqrt{\frac{\pi}{2\Delta}} e^{\frac{3\Gamma^2}{4\Delta^2}} \text{Bessel} K(0, \frac{3\Gamma^2}{4\Delta^2})$$

$$(\text{when} \quad \Phi_{pr}(\omega_{pr}) = \arctan(\omega_{pr}/\Gamma) + \text{cons})$$

Here K is a modified Bessel function. Thus the optimal phase to enhance the resonant signal is $\Phi_{pr}(\omega_{pr}) = \arctan(\omega_{pr}/\Gamma) + \text{cons}$ with pump and Stokes pulses being unshaped transform limited pulses (TLPs). While for the non-resonant background, we have $P_{nr}^{(3)} = \chi_{nr} \sqrt{\frac{\pi}{2\Delta}} \int_{-\infty}^{\infty} d\omega_{pr} e^{-\frac{3\omega_{pr}^2}{2\Delta^2}} e^{i(\Phi_{pr}(\omega_{pr}))}$.

So the non-resonant background will reach its minimal value of zero when $\Phi_{pr}(\omega_{pr})$ is the Π step phase function about $\omega_{pr} = 0$.

Case 2: the pump pulse is also used as the probe pulse in two-pulse CARS, and phase shaping of the pump pulse is conducted to maximize the resonant signal at $\omega_{as} = 0$. In this case, the resonant signal is

$$P_r = \frac{1}{\Delta^{3.2}} \int_{-\infty}^{\infty} \frac{C}{\omega_{pr} - i\Gamma} e^{-\frac{3\omega_{pr}^2}{2\Delta^2} + i\Phi_p(\omega_{pr})} \int_{-\infty}^{\infty} e^{-\frac{2(\omega_p + \omega_{pr}/2)^2}{2\Delta^2} + i\Phi_p(\omega_{pr})} d\omega_p d\omega_{pr} .$$

The numerical solution in Figure 5 shows that the optimal phase function is approximately a superposition of the linear and $\arctan(\omega_{pr}/\Gamma)/2$ phases: the optimal phase is quasi-linear away from $\omega_p = 0$ and similar to $\arctan(\omega_{pr}/\Gamma)/2$ around $\omega_p = 0$. This can be understood as follows: since the zero phase profile (linear) is optimal for $| \int_{-\infty}^{\infty} e^{-\frac{2(\omega_p + \omega_{pr}/2)^2}{2\Delta^2} + i\Phi_p(\omega_{pr})} d\omega_p |$, and the $\arctan(\omega_p/\Gamma)$ phase is optimal for

$| \int_{-\infty}^{\infty} \frac{C}{\omega_{pr} - i\Gamma} e^{-\frac{3\omega_{pr}^2}{2\Delta^2} + i\Phi_p(\omega_{pr})} d\omega_{pr} |$, then an approximate superposition of the linear and

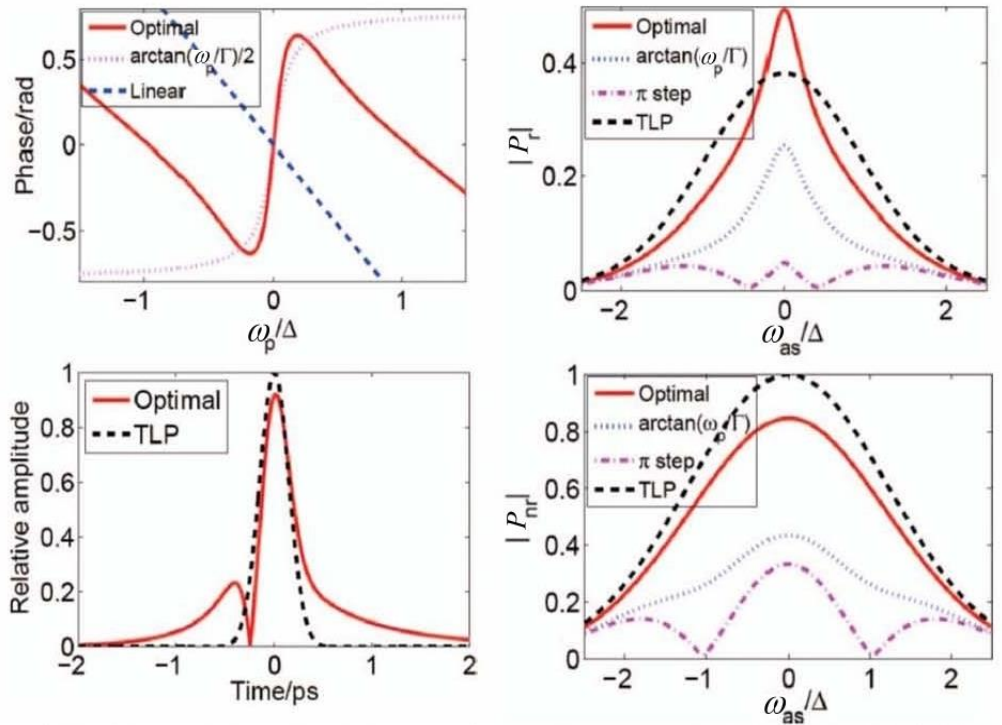$\arctan(\omega_p / \Gamma)$ functions will maximize $| P_r |$.

Figure 5. The left panel: the optimal phase function for the pump pulse in two-pulse CARS. They are shown together with different shaping strategies in the frequency and time domains, respectively. TLP means transform limited pulse (no phase shaping). The right panel: the resonant signal and non-resonant background spectra with different phase shaping schemes for the pump pulse in two-pulse CARS. The parameters are $\Delta = 50\text{cm}^{-1}, \Gamma = 4.8\text{cm}^{-1}$. Reproduced from [Gao et al, 2012], with the permission of AIP Publishing.

Case 3: The probe pulse is shaped to control the signal-background difference at $\omega_{as} = 0$. In the lab, the signal and background are always detected together. Thus we have to enhance the resonant signal and suppress the non-resonant background simultaneously, which is a multi-objective optimization problem. It is better to choose the signal-background difference as the objective functional than the signal-to-background ratio, since the ratio will become infinite when $|P_{nr}| = 0$ no matter how small $|P_r|$ is. A weight factor can be introduced to place different importance on background elimination: $J = | P_r |^2 - k | P_{nr} |^2$.

With the variational method, the optimal phase for the probe pulse is

$$\Phi_{pr}(\omega_{pr}) = \arctan\left(\frac{\omega_{pr}}{\Gamma - \lambda\gamma(\omega_{pr}^2 + \Gamma^2)}\right) + \theta$$

Here $\lambda = k(\chi_{nr}/C)^2$, and γ can be determined by iteratively solving the equation

$$\gamma = \frac{\int_{-\infty}^{\infty} e^{-\frac{3x^2}{2\Delta^2}} \cos(\arctan(\frac{x}{\Gamma - \lambda\gamma(x^2 + \Gamma^2)}))dx}{\int_{-\infty}^{\infty} e^{-\frac{3x^2}{2\Delta^2}} \frac{1}{\sqrt{x^2 + \Gamma^2}} \sin(\arctan(\frac{x}{\Gamma - \lambda\gamma(x^2 + \Gamma^2)}) - \arctan(\frac{\omega_{pr}}{\Gamma}) + \frac{\pi}{2})dx}$$

Case 4: All the three pulses can be shaped for broadband signal enhancement and background suppression. The control here is broadband optimal control. In this case, the following objective functional can be adopted

$$J = I_r - I_{nr} = \int_{-\infty}^{\infty} |P_r|^2 d\omega_{as} - \int_{-\infty}^{\infty} |P_{nr}|^2 d\omega_{as}.$$
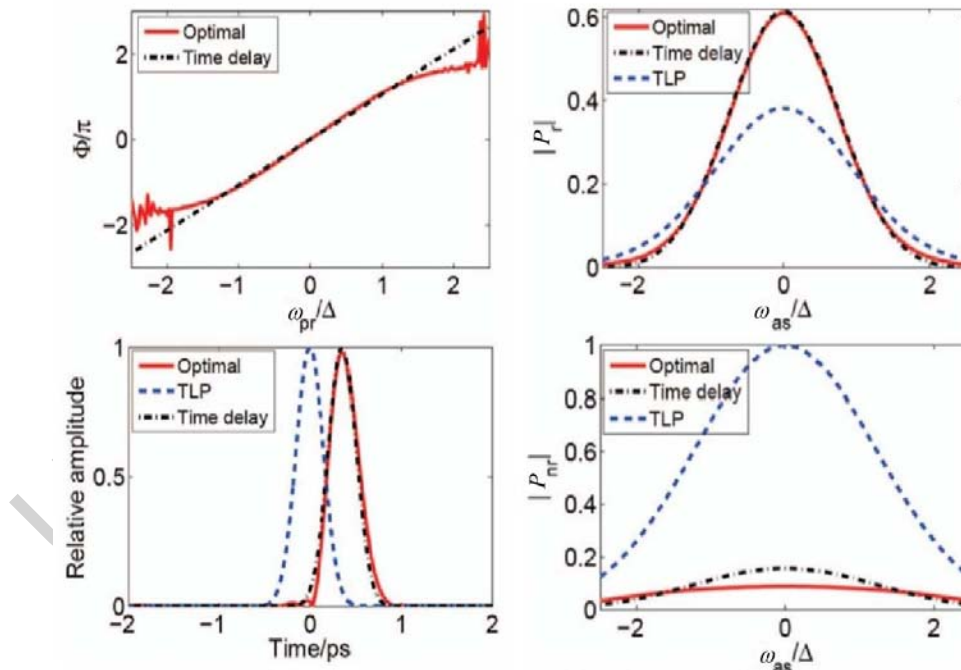

Figure 6. The left panal: the optimal phase function for the probe pulse in broadband optimal control. They are shown together with different shaping strategies in the frequency and time domains, respectively. TLP means transform limited pulse (no phase shaping). The right panel: the resonant signal and non-resonant background spectra with different phase shaping schemes for the probe pulse in three-pulse CARS. The parameters are $\Delta = 50 \text{cm}^{-1}, \Gamma = 4.8 \text{cm}^{-1}$. Reproduced from [Gao et al, 2012], with the permission of AIP Publishing.

Analytical solution is not possible here, and numerical simulations show that the optimal phase shaping configuration consists of unshaped pump and Stokes pulses and a shaped probe pulse as shown in Figure 6.

It can be seen that the time delay scheme, which is usually adopted in the experiments, has almost the best performance in suppressing the broadband non-resonant background.

-

-

-

Bibliography

Weiner A. M., Femtosecond pulse shaping using spatial light modulators, Review of Scientific Instruments, Vol. 71, No. 5, pp. 1929-1960 (2000) [After outlining the fundamental principles of pulse shaping methods, author presents a detailed discussion of pulse shaping using several different types of spatial light modulators. Applications of pulse shaping to optical communications, biomedical optical imaging, high power laser amplifiers, quantum control, and laser-electron beam interactions are reviewed.]

Brif C., Chakrabarti R., Rabitz H., Control of quantum phenomena: past, present and future, New Journal of Physics, Vol. 12, No. 7, pp. 075008 (2010) [This work presents a perspective of progress in the field of control over quantum phenomena, tracing the evolution of theoretical concepts and experimental methods from early developments to the most recent advances. Among numerous theoretical insights and technological improvements that produced the present state-of-the-art in quantum control, there have been several breakthroughs of foremost importance. The subjects discussed include quantum optimal control theory, quantum control landscapes, the role of theoretical control designs in experimental realizations and real-time quantum feedback control.]

Goswami D., Optical pulse shaping approaches to coherent control, Physics Reports, Vol. 374, No. 6, pp. 385-481 (2003) [This review captures certain aspects and impacts of optical pulse shaping into the fast developing areas of coherent control and other related fields. Currently available reviews focus on one or the other detailed aspects of coherent control, and the reader will be referred to such details as and when necessary for issues that are dealt in brief here.]

Weiner A. M., Ultrafast optical pulse shaping: A tutorial review, Optics Communications, Vol. 284, No. 15, pp. 3669-3692 (2011) [This paper presents a tutorial on the field of femtosecond pulse shaping, a technology that enables generation of nearly arbitrary, user defined, ultrafast optical waveforms, with control of phase, amplitude, and polarization.]

Duncan M. D., Reintjes J., Manuccia T. J., Scanning coherent anti-stokes raman microscope, Optics Letters, Vol. 7, No. 8, pp. 350-352 (1982) [The authors have constructed scanning coherent anti-Stokes Raman spectroscopic apparatus that allows to image the distribution of distinct chemical species in a microscopic sample region.]

Cheng J. X., Volkmer A., Xie X. S., Theoretical and experimental characterization of coherent anti-stokes raman scattering microscopy, Journal of the Optical Society of America B, Vol. 19, No. 6, pp. 1363-1375 (2002) [Experimental implementations of CARS microscopy with collinearly co-propagating and counter-propagating excitation beams, forward and backward data collection, and polarization-sensitive detection are described.]

Judson R. S., Rabitz H., Teaching lasers to control molecules, Physical Review Letters, Vol. 68, pp. 1500-1503 (1992) [The authors simulate a method to teach a laser pulse sequences to excite specified molecular states. We use a learning procedure to direct the production of pulses based on ''fitness'' information provided by a laboratory measurement device. Over a series of pulses the algorithm learns an optimal sequence. The experimental apparatus, which consists of a laser, a sample of molecules and a measurement device, acts as an analog computer that solves Schrödinger's equation exactly, in real time.]

Rabitz H., Regina de Vivie-Riedle, Motzkus M., Kompa K., Whither the future of controlling quantum phenomena?, Science, Vol. 288, No. 5467, pp. 824-828 (2000) [This review puts into perspective the present state and prospects for controlling quantum phenomena in atoms and molecules. The topics considered include the nature of physical and chemical control objectives, the development of possible quantum control rules of thumb, the theoretical design of controls and their laboratory realization, quantum learning and feedback control in the laboratory, bulk media influences, and the ability to utilize coherent quantum manipulation as a means for extracting microscopic information.]

Gao F., Shuang F., Shi J., Rabitz H., Wang H., Cheng J. X., Optimal coherent control of coherent anti-stokes raman scattering: Signal enhancement and background elimination, The Journal of Chemical Physics, Vol. 136, No. 14 pp. 144114 (2012) [The ability to enhance resonant signals and eliminate the non-resonant background is analyzed for coherent anti-Stokes Raman scattering. The analysis is done at a specific frequency as well as for broadband excitation using femtosecond pulse-shaping techniques.]

Liu C., Kim D. Y., Differential imaging in coherent anti-stokes raman scattering microscopy with laguerre- gaussian excitation beams, Optics Express, Vol. 15, No. 16, pp. 10123-10134 (2007) [A new differential imaging technique is proposed to visualize the fine structures and the edges of a sample in coherent anti-Stokes Raman Scattering (CARS) microscopy. Both the pump and Stokes excitation fields are modulated simultaneously with a spiral phase mask which transforms them from Gaussian modes into Laguerre-Gaussian modes of LG01 for CARS excitation. It is much suitable for visualizing structures with a scale comparable to the excitation wavelength and has higher reliability in retrieving chemical structural information of the sample compared to common CARS microscopy.]

Krishnamachari V. V., Potma E. O., Focus-engineered coherent anti-stokes raman scattering microscopy: a numerical investigation, Journal of the Optical Society of America A, Vol. 24, No. 4, pp. 1138-1147 (2007a) [The authors presented numerical investigation of focus-engineered coherent anti-Stokes Raman scattering microscopy.]

Krishnamachari V. V., Potma E. O., Detecting lateral interfaces with focus-engineered coherent anti-stokes raman scattering microscopy, Journal of Raman Spectroscopy, Vol. 39, No. 5, pp. 593-598 (2008) [Detecting lateral interfaces with focus-engineered coherent anti-Stokes Raman scattering microscopy is presented.]

Krishnamachari V. V., Potma E. O., Imaging chemical interfaces perpendicular to the optical axis with focus-engineered coherent anti-stokes raman scattering microscopy, Chemical Physics, Vol. 341, No. 1-3, pp. 81-88 (2007b) [The authors apply the concept of focus engineering to enhance the sensitivity of coherent anti-Stokes Raman scattering microscopy to vibrational microscopy. Based on detailed numerical simulations, it was shown that using a focused Stokes field with a sharp phase jump along the longitudinal direction leads to the suppression of the signal from bulk regions and improves the signal contrast from vibrational resonant interfaces oriented perpendicular to the axis of beam propagation.]

Wang P., Slipchenko M. N., Mitchell J., Yang C., Potma E. O., Xu X., Cheng J. X., Far-field imaging of non-fluorescent species with subdiffraction resolution, Nature Photonics, Vol. 7, No. 6, pp. 450-454 (2013) [A scheme for breaking the diffraction limit in far-field imaging of non-fluorescent species by using spatially controlled saturation of electronic absorption is demonstrated. The method is based on a pump-probe process where a modulated pump field perturbs the charge-carrier density in a sample, thus modulating the transmission of a probe field. This technique potentially enables super-resolution imaging of nano-materials and non-fluorescent chromophores, which may remain out of reach for fluorescence-based methods.]

Roth M., Guyon L., Roslund J., Boutou V., Courvoisier F., Wolf J. P., Rabitz H., Quantum control of tightly competitive product channels, Physical Review Letters, Vol. 102, pp. 253001 (2009) [Fundamental selectivity limits of quantum control are pushed by introducing laser driven optimal dynamic discrimination to create distinguishing excitations on two nearly identical flavin molecules. Even

with modest spectral resources, significant specificity is achieved with optimal pulse shapes, which amplify small molecular differences to create distinct, identifying signals.]

Petersen J., Mitrić R., Bonačić-Koutecký V., Wolf J. P., Roslund J., Rabitz H., How shaped light discriminates nearly identical biochromophores, Physical Review Letters, Vol. 105, pp. 073003 (2010) [A general mechanism for successful discrimination of spectroscopically indistinguishable biochromophores by shaped light is presented. For this purpose nonadiabatic dynamics in excited electronic states in the frame of the field-induced surface hopping method driven by the experimentally shaped laser fields is used. The presented mechanism leads to selective fluorescence depletion which serves as a discrimination signal.]

Mitra A. , Solá I. R., Rabitz H., Revealing quantum-control mechanisms through hamiltonian encoding in different representations, Physical Review A, Vol. 67, pp. 043409 (2003) [Revealing quantum control mechanisms through Hamiltonian encoding in different representation are discussed.]

Mitra A., Solá I. R., Rabitz H., Understanding the role of respresentation in controlled quantum-dynamical mechanism analysis, Physical Review A, Vol. 77, pp. 043415 (2008) [In this work the choice of representation is set up as the solution to a variational optimization problem. For unconstrained basis transformations, the optimization of the representation is formally equivalent to solving the time-dependent Schrödinger equation; different constrained basis transformations provide distinct dynamical perspectives.]

Mitra A., Rabitz H., Identifying mechanisms in the control of quantum dynamics through hamiltonian encoding, Physical Review A, Vol. 67, pp. 033407 (2003) [This paper proposes a method to quantitatively determine the various pathways taken by a quantum system in going from the initial state to the final target. The mechanism is revealed by encoding a signal in the system Hamiltonian and decoding the resultant nonlinear distortion of the signal in the system time-evolution operator. The relevant interfering pathways determined by this analysis give insight into the physical mechanisms operative during the evolution of the quantum system. The mechanism identification concept is presented in the context of analyzing computer simulations of controlled dynamics. As illustrations of the concept, mechanisms are identified in the control of several simple, discrete-state quantum systems.]

Mitra A., Rabitz H., Quantum control mechanism analysis through field based Hamiltonian encoding, The Journal of Chemical Physics, Vol. 125, No. 19, pp. 194107 (2006) [This work introduces the scheme of field based HE, where the modulation is encoded into the control field and not directly into the Hamiltonian operators. This distinct form of modulation yields a new perspective on mechanism and is computationally faster than the earlier approach. This new hierarchical algorithm is an improvement over earlier approaches to HE where the entire mechanism was determined in one stroke. A number of simulations are presented on simple systems to illustrate the new field based encoding technique for mechanism assessment.]

Mitra A., Rabitz H., Quantum control mechanism analysis through field based Hamiltonian encoding: A laboratory implementable algorithm, The Journal of Chemical Physics, Vol. 128, No. 4, pp. 044112 (2008) [As a step towards laboratory implementation of Hamiltonian encoding, the authors addresses the issues raised by the use of observables rather than the wave function in HE. The proposed algorithm can handle complex systems, operates with no recourse to dynamical simulations, and functions with limited understanding of the system Hamiltonian. As with the closed-loop control experiments, the HE control mechanism identification algorithm performs a new experiment each time the dynamical outcome from an encoded Hamiltonian is called for. This paper presents the basic HE algorithm in the context of physical systems described by a finite dimensional Hilbert space.]

Rey-de Castro R., Leghtas Z., Rabitz H., Manipulating quantum pathways on the fly, Physical Review Letters, vol. 110, pp. 223601 (2013a) [The authors demonstrate for the fist time adaptive manipulation of quantum pathways using the Hamiltonian encoding-observable decoding (HE-OD) technique. The principles of HE-OD are illustrated for population transfer in atomic rubidium using shaped femtosecond laser pulses.]

Rey-de Castro R., Cabrera R., Bondar D. I., Rabitz H., Time-resolved quantum process tomography using Hamiltonian-encoding and observable-decoding, New Journal of Physics, Vol. 15, No. 2, pp. 025032 (2013b) [The Hamiltonian encoding observable decoding (HE-OD) technique is experimentally demonstrated for process tomography of laser-induced dynamics in atomic Rb vapor. With the assistance of a laser pulse truncation method, a time dependent reconstruction of the quantum evolution is achieved.]

Biographical Sketches

Feng Shuang graduated from University of Science and Technology of China as a Ph.D in chemical physics in 2000. Then he worked as a post-doctoral researcher at Hong Kong University of Science and Technology. After that, he went to Princeton University as a post-doctoral research associate from 2001 to 2003, and then became a research staff member at Princeton University after 2004. In 2009, he was admitted into One Hundred Talent Program in Chinese Academy of Sciences, and worked as a professor at Institute of Intelligent Machines, Chinese Academy of Sciences. He is now the director of Robot Sensor and Human-Machine Interaction Laboratory at IIM. His main researches cover tactile sensors, quantum sensors, information acquisition, quantum control, and quantum measurement. His studies have shown some new insights on quantum control, such as the optimal quantum measurement and the effect of noises and environment to quantum control. Number of his scientific publications is more than 50

Jixin Cheng carried out his PhD study in University of Science and Technology of China from 1994 to 1998.. After postdoctoral training in Yijing Yan's group at Hong Kong University of Science and Technology and Sunney Xie's group at Harvard University, Cheng joined Purdue University in 2003 as Assistant Professor. He was promoted to Associate Professor in 2009 and Full Professor in 2013 in the Weldon School of Biomedical Engineering and Department of Chemistry. His research lab develops label-free spectroscopic imaging tools and nanotechnologies for challenging applications in biology and medicine. His research has yielded over 140 peer-reviewed articles that have been cited more than 7000 times. His contribution to the research field is demonstrated as the organizer of 16 national symposia, over 120 invited talks, and as primary editor of the first book on Coherent Raman Scattering Microscopy (2012). His is a co-inventor of CARS microscopy which is now available through Olympus and Leica.

Fang Gao graduated from University of Science and Technology of China in 2010, earning his Ph.D in chemical physics. After that, he worked as an assistant professor at Institute of Intelligent Machines. In 2013, he was promoted to an associate professor. His research interests mainly focus on quantum sensors, quantum control and computation chemistry. He has successfully carried out studies on optimal coherent control of CARS (coherent anti-Stokes Raman scattering) and pathway dynamics in the optimal quantum control of rubidium. Number of scientific publications is more than 20.

Yaoxiong Wang graduated from Northwestern University (China) in 2009, with a master degree in physics. After that, he joined Institute of Intelligent Machines, and became an assistant professor from 2012. His research interest includes quantum measurement, quantum control and compressive sensing. He has studied the optimal quantum measurement of finite-dimensional systems and perfect state transfer in spin chains. Number of scientific publications is more than 10.

Dewen Cao is now a Ph.D student under the supervision of Prof. Feng Shuang. His research mainly includes quantum control and quantum dissipation theory.